A hierarchical approach for online temporal lobe seizure detection in long-term intracranial EEG recordings

2013 J. Neural Eng. 10 045004

(http://iopscience.iop.org/1741-2552/10/4/045004)

J. Neural Eng. **10** (2013) 045004 (14pp) doi:10.1088/1741-2560/10/4/045004

A hierarchical approach for online temporal lobe seizure detection in long-term intracranial EEG recordings

Sheng-Fu Liang[1,2,6], **Yi-Chun Chen**[2], **Yu-Lin Wang**[3], **Pin-Tzu Chen**[2], **Chia-Hsiang Yang**[4] **and Herming Chiueh**[5]

[1] Institute of Medical Informatics, National Cheng Kung University, Tainan, Taiwan
[2] Department of Computer Science and Information Engineering, National Cheng Kung University, Tainan, Taiwan
[3] Biomedical Electronics Translational Research Center, National Chiao Tung University, Hsinchu, Taiwan
[4] Department of Electronics Engineering, National Chiao Tung University, Hsinchu, Taiwan
[5] Department of Electrical Engineering, National Chiao Tung University, Hsinchu, Taiwan

E-mail: sfliang@mail.ncku.edu.tw

Received 28 March 2013
Accepted for publication 22 April 2013
Published 31 May 2013
Online at stacks.iop.org/JNE/10/045004

Abstract

Objective. Around 1% of the world's population is affected by epilepsy, and nearly 25% of patients cannot be treated effectively by available therapies. The presence of closed-loop seizure-triggered stimulation provides a promising solution for these patients. Realization of fast, accurate, and energy-efficient seizure detection is the key to such implants. In this study, we propose a two-stage on-line seizure detection algorithm with low-energy consumption for temporal lobe epilepsy (TLE). *Approach.* Multi-channel signals are processed through independent component analysis and the most representative independent component (IC) is automatically selected to eliminate artifacts. Seizure-like intracranial electroencephalogram (iEEG) segments are fast detected in the first stage of the proposed method and these seizures are confirmed in the second stage. The conditional activation of the second-stage signal processing reduces the computational effort, and hence energy, since most of the non-seizure events are filtered out in the first stage. *Main results.* Long-term iEEG recordings of 11 patients who suffered from TLE were analyzed via leave-one-out cross validation. The proposed method has a detection accuracy of 95.24%, a false alarm rate of 0.09/h, and an average detection delay time of 9.2 s. For the six patients with mesial TLE, a detection accuracy of 100.0%, a false alarm rate of 0.06/h, and an average detection delay time of 4.8 s can be achieved. The hierarchical approach provides a 90% energy reduction, yielding effective and energy-efficient implementation for real-time epileptic seizure detection. *Significance.* An on-line seizure detection method that can be applied to monitor continuous iEEG signals of patients who suffered from TLE was developed. An IC selection strategy to automatically determine the most seizure-related IC for seizure detection was also proposed. The system has advantages of (1) high detection accuracy, (2) low false alarm, (3) short detection latency, and (4) energy-efficient design for hardware implementation.

(Some figures may appear in colour only in the online journal)

[6] Author to whom any correspondence should be addressed.

1. Introduction

Epilepsy is one of the most common neurological disorders, and temporal lobe epilepsy (TLE) is probably the most common focal epilepsy in humans (Engel, 1989). TLE consists of simple partial seizures without loss of awareness and complex partial seizures (i.e. with loss of awareness). Through treatment with antiepileptic drugs (AEDs), about 75% patients can be treated. However, the side effects and safety issues associated with the use of AEDs are still of concern (Stacey and Litt, 2008). Alternative techniques, such as vagus nerve stimulation (VNS; Labar *et al* 1999) and deep brain stimulation (DBS; Chabardes *et al* 2002) have been proposed for open-loop seizure control. However, the efficacy of intermittent stimulation may decrease due to neuron acclimation (Politsky *et al* 2005, Raghunathan *et al* 2009). Therefore, a closed-loop device can suppress seizure events more efficiently than an open-loop seizure controller by activating the electrical stimulator once a seizure event is detected (Stacey and Litt, 2008, Kossoff *et al* 2004).

An essential technique required for closed-loop seizure control is robust, on-line seizure detection that can drive effective antiepileptic stimulations in the very early stage when seizures occur. Various techniques developed for seizure detection over long-term continuous electroencephalogram (EEG) recordings have been developed by leveraging line length (Esteller *et al* 2001), data range autocorrelation considering spike frequency (White *et al* 2006), combination of approximate entropy and spectral sub-bands (Liang *et al* 2010), fuzzy-rule based classification (Aarabi *et al* 2009), nonlinear dimension reduction via wavelet transform (Zhang *et al* 2010), wavelet filtering (Osorio *et al* 2002), Davies–Bouldin (DB) indexing (Wilson, 2006), and high frequency activities in wavelet domain (Ayoubian *et al* 2013). The design goal is to achieve high detection accuracy, a low false alarm rate, and a short delay time. A seizure detection algorithm that can be implemented efficiently is also necessary for portable devices (Raghunathan *et al* 2009, Liang *et al* 2011, Young *et al* 2011). The effectiveness of the on-line detection algorithms needs to be verified on continuous EEG data.

Movement artifacts are serious problems in EEG analysis. The performance of seizure detection is usually degraded significantly due to the artifacts. Independent component analysis (ICA) is one promising solution to eliminate artifacts and extract meaningful signals when applied to EEG (McMenamin *et al* 2010, Kocyigit *et al* 2008). Although ICA can be used to separate artifacts from the source signals, the computational complexity after ICA is very high. The identical algorithm needs to be applied to all independent components (ICs) (Chang *et al* 2010, Subasi and Gursoy 2010) and it may take a considerable amount of computation time for seizure detection. The selection of the significant ICs are now determined manually (LeVan *et al* 2006). An algorithm for automatically determining the most seizure-related component therefore becomes necessary.

For implantable or wearable devices, the battery life of such a detection system becomes important. In this study, we have developed a hierarchical seizure detection method that has low computational complexity and high detection accuracy for closed-loop seizure control devices. The long-term intracranial EEG (iEEG) recordings of 11 patients suffering from temporal lobe seizures were analyzed. ICA is first applied to remove the artifacts. The IC which has the most ictal activity is determined automatically. The processing time required for seizure detection is reduced by using the selected IC. In the first stage, two temporal features of a segment are evaluated. If the segment is considered as a non-seizure, the current segment is rendered up. When a suspected segment is found, the second-stage detection is activated. In the second stage, we use two metrics as the input vectors of a linear classifier for confirmation. With this two-stage seizure detection algorithm, the computational complexity is reduced, thereby reducing the energy dissipation. In this way, the sustainability of the closed-loop seizure control system can be improved by the proposed method, and therefore the patients' quality of life can be enhanced as well.

2. Material and methods

2.1. Datasets

The iEEG data used in this study were obtained from the Freiburg Seizure Prediction EEG database (Freiburg Seizure Prediction Project, 2008). In this study, the iEEG recordings of 11 epileptic patients who suffered from TLE were used to test the detection performance. All of the data were recorded during pre-surgical monitoring at the Epilepsy Center of the University Hospital of Freiburg, Germany. The iEEG data were acquired using a 128-channel Neurofile NT digital video iEEG system with 16-bit resolution at a 256 Hz sampling rate. Data were filtered by a 0.5–100 Hz band-pass filter, and a 50 Hz notch filter was applied to remove power-line noise. For each patient, only six channels of recordings were released. Three channels were selected from the seizure onset zone (i.e. from areas involved early in ictal activity, in-focus electrodes; Aschenbrenner-Scheibe *et al* 2003). The remaining three channels were selected from the out-focus area. There are 42 seizures in the iEEG recordings of 11 patients. Details of the patients' characteristics are listed in table 1.

2.2. Seizure detection algorithm

The detection flow chart of the proposed hierarchical method is shown as figure 1. To reduce the interference of artifacts, ICA is first applied to multi-channel iEEGs. The IC that has the most ictal activity is determined for further analysis. The signals of the determined IC are divided into 512-point segments with an overlap of 384 points. Each segment is visually labeled as one of three possible behavioral states: normal, seizure, or artifact. In the training phase, the features of segments are grouped according to their behavioral states. Those features are utilized for training the classification model.

The feature index of each segment is extracted and analyzed for the two-stage seizure detection. When a suspected segment is detected, the second stage is activated for final confirmation. Meanwhile, a temporal constraint *Nc* is used to reduce the false alarm rate. If the number of

Table 1. Characteristics of 11 patients with TLE.

Patient	Gender	Age	Seizure type	Origin	Electrode type	Resection outcome	Number of seizures	Average seizure duration (s)
2	M	38	SP,CP,GTC	H	D	IV	3	118.2
4	F	26	SP,CP,GTC	H	d, g, s	No surgery	5	87.4
6	F	31	CP,GTC	H	d, g, s	I	3	66.9
7	F	42	SP,CP,GTC	H	D	I	3	153.5
11	F	10	SP,CP,GTC	NC	g, s	II	4	91.1
12	F	42	SP,CP,GTC	H	d, g, s	IV	4	55.1
13	F	22	SP,CP,GTC	H	d, s	II	2	158.3
14	F	41	CP,GTC	H, NC	d, s	I	4	216.4
15	M	31	SP,CP,GTC	H, NC	d, s	III	4	89.6
17	M	28	SP,CP,GTC	NC	S	I	5	86.2
21	M	13	SP,CP	NC	g, s	I	5	83.1
Average	X	29.5	X	X	X	X	3.8	109.6

Resection outcome according to Engel classification. Gender: F = female; M = male. Seizure type: SP = simple partial; CP = complex partial; GTC = generalized tonic–clonic. Origin: H = hippocampal; NC = neocortical; FT = frontal. Electrode types: g = electrodes grid; s = strip; d = depth.

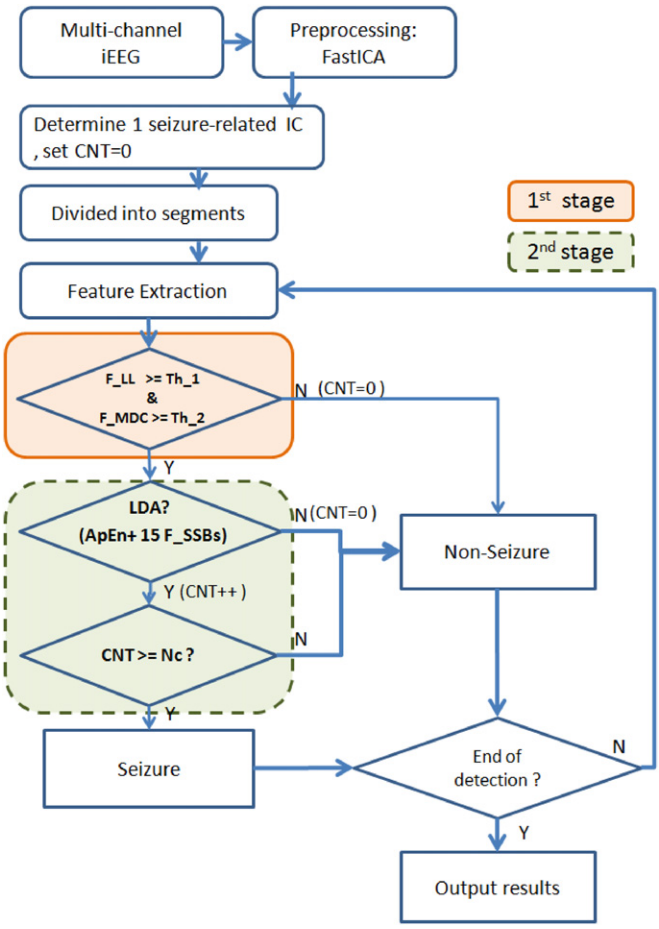

Figure 1. Flow chart of the proposed hierarchical method. ICA is first applied to multi-channel iEEG recordings. The first stage evaluates each segment with a low-complexity algorithm in order to operate in a low-power mode. The second stage stays idle until a suspected seizure segment is found. The steps repeat until all segments are analyzed.

consecutive segments classified as seizure states by the second stage reaches approaches *Nc*, the system will report that a seizure event occurs. The system repeats the detection steps until all segments were analyzed. The details of the operations are elaborated in the next sections.

2.3. Preprocessing

Our experiment is performed in two phases: training and testing. In the training phase, we apply ICA to determine the mixing matrix $\boldsymbol{A}$ for each patient. In the testing phase, the obtained matrix $\boldsymbol{A}$ is used to decompose a subject's iEEG signals so that the most seizure related IC can be derived without computing ICA again.

Fast ICA (FastICA; Hyvärinen, 1999) is used for signal separation due to its robustness, low computational complexity, and fast convergence. It has been commonly used to remove artifacts and extract seizure components for seizure identification (Jung *et al* 2000, Kocyigit *et al* 2008). Since only six iEEG channels (three from in-focus electrodes and three from out-focus electrodes) are released, the proposed approach is developed based on six channel recordings.

Notations used in this paper are elaborated as follows.

(1) $X = [x_1, \ldots, x_6]^T$: the 6-channel iEEG signals.
(2) $Y = [y_1, \ldots, y_6]^T$: the six ICs after ICA decomposition.
(3) $A = [a_{ij}]_{6\times 6}$: a mixing matrix, and $X = AY$. The entries of ith column of A stand for the projection lengths of ith IC onto respective iEEG channels, which also represents the contribution of ith IC to the total variation of the 6-channel iEEGs signals.
(4) α, β and γ : the three iEEG channels that are closest to the seizure onset zone, where $1 \leqq \alpha, \beta, \gamma \leqq 6$ and $\alpha \neq \beta \neq \gamma$.

For each patient, the automatic IC determination steps are described as follows.

(1) α, β and γ are derived in advance from patient's basic characteristics (table 1).
(2) 6-channel iEEGs X are decomposed into 6 ICs Y and mixing matrix A through FastICA.
(3) For ith IC, we calculate the weighted sum of entries corresponding to α, β and γ channels, and further compute its ratio over all entries (6 channels). The resulting ratio R_i is formulated as (1), and it also represents that the density of ictal activities of seizure onset zone contributed by the ith IC.

$$R_i = \frac{\sum_{k=\alpha,\beta,\gamma} a_{ik}}{\sum_{k=1}^{6} a_{ik}} \quad (1)$$

(4) The IC that has the maximal R value is chosen. That is, the IC that has the highest density of ictal activity in the seizure onset zone is determined for seizure detection.

It is noted that the concept of the proposed IC selection strategy is to analyze the density of ictal activities and to select the IC with the strongest projection in the seizure onset zone. Because only the data from six iEEG channels are released in the utilized dataset, the proposed method is developed based on six-channel recordings but not limited to six channels.

2.4. First stage for fast suspect detection

Extracting feature indexes of each segment is essential for determining whether a particular iEEG segment is in a seizure-like state. The design principle of the first stage is to detect the suspected segment with a short delay time. The first stage is therefore named the fast suspect detection stage. Two temporal features, line length analysis and Hjorth parameters, are utilized to detect the behavioral state of the iEEG segment. When the feature values are greater than their respective thresholds, the second stage is activated. This conditional activation allows for considerable energy savings.

2.4.1. Line length analysis. Line length analysis was first proposed by Esteller *et al* (2001) for seizure detection. It is sensitive to the variations of amplitude and frequency in signals, and is treated as a measure of 'seizureness' or the pathology of the combined amplitude–frequency characteristics of the EEGs (Esteller *et al* 2004). Given a time series $x(n)$, $n = 1, \ldots, N$, the line length (F_LL) is defined by the sum of the lengths of the line segments between successive samples of a signal:

$$F\_LL = \sum_{i=1}^{N-1} \text{abs}\,[x(i+1) - x(i)]. \tag{2}$$

Figure 2 shows two examples of iEEG waveforms after applying line length analysis. Figure 2(a) first shows a segment of the original waveforms with one seizure event of patient#6, and the next row displays the corresponding F_LL values. The dotted (solid) line indicates the time of seizure onset (end) of seizures. It shows that the value of F_LL becomes greater during the seizure period. F_LL is also sensitive to amplitude and frequency variations in the signals. An example is shown in figure 2(b) where the other segment is affected seriously by artifacts. It shows the F_LL has greater values for artifacts. Figure 2(c) shows the histogram of F_LL for all patients. Although F_LL is a good index to discriminate the seizure segments from normal segments, it is still difficult to distinguish between artifact segments and seizure segments using only F_LL. Therefore, one more parameter, F_MDC, evolved from Hjorth analysis, is added to improve the correctness and efficiency.

2.4.2. Hjorth analysis. Hjorth parameters (Hjorth, 1970) have been extensively used in time-domain EEG analysis (Indiradevi *et al* 2009, Päivinen *et al* 2005). Given a time series x, three parameters, *Activity*, *Mobility*, and *Complexity*, are defined as (3) to (5), respectively:

$$\text{Activity} = \sigma_x^2 \tag{3}$$

$$\text{Mobility} = \frac{\sigma_{x'}}{\sigma_x} \tag{4}$$

$$\text{Complexity} = \frac{\sigma_{x''}/\sigma_{x'}}{\sigma_{x'}/\sigma_x}, \tag{5}$$

where σ_x,$\sigma_{x'}$ and $\sigma_{x''}$ are the standard deviations of the original, first, and second derivatives of the iEEG signals.

In this paper, we propose a new feature, F_MDC, the ratio between *Mobility* and *Complexity*, for fast suspect detection:

$$F\_MDC = \frac{\text{Mobility}}{\text{Complexity}}. \tag{6}$$

Taking patient #21 for illustration, we calculate the three Hjorth parameters and F_MDC of the iEEG signals. Figure 3(a) first shows the original iEEG waveforms with one seizure event. The dotted (solid) line indicates the onset (end) of the seizure. The second to fifth rows illustrate the values of *Activity*, *Mobility*, *Complexity* and the new proposed feature, F_MDC, respectively. From the sub-figures, it can be seen that the fluctuation of *Activity* is the most insignificant during a seizure event. For a seizure event, the *Mobility* increases, while *Complexity* decreases. F_MDC (*Mobility* divided by *Complexity*) during seizure is steadily greater than that during inter-ictal period. Figure 3(b) displays the histograms of four Hjorth parameters of normal, seizure and artifact segments. It is shown that 'F_MDC' has the smallest overlap between seizure and non-seizure segments. F_LL and F_MDC are therefore used to detect the suspected segments in the first stage.

2.4.3. Determination on two thresholds. The decisive features of a segment used for detecting a suspected seizure segment are determined by (7) and (8), where two thresholds are denoted as Th_1 and Th_2, respectively. If F_LL and F_MDC of a segment are both greater than their respective thresholds, the segment is marked as a suspected seizure segment. The second stage is then activated for final confirmation:

$$Th\_1 = \text{Avg}[F\_LL] - \text{Std}[F\_LL] \tag{7}$$

$$Th\_2 = \text{Avg}[F\_MDC] - \text{Std}[F\_MDC] \tag{8}$$

where Avg[·] and Std[·] stand for the average and standard deviation, respectively.

2.5. Second stage of seizure confirmation

In the second stage, we use two metrics as input vectors into a linear discriminant analyzer (LDA) for the final seizure confirmation. The two metrics are from the approximate entropy (*ApEn*) analysis proposed by Pincus (Pincus 1991) and from EEG power spectrum analysis. In our previous study (Liang *et al* 2010), it was observed that combining *ApEn* with the multi-band EEG power spectra can effectively classify the ictal and non-ictal EEG segments. In this work, this approach is further utilized for seizure detection in long-term continuous iEEG signals.

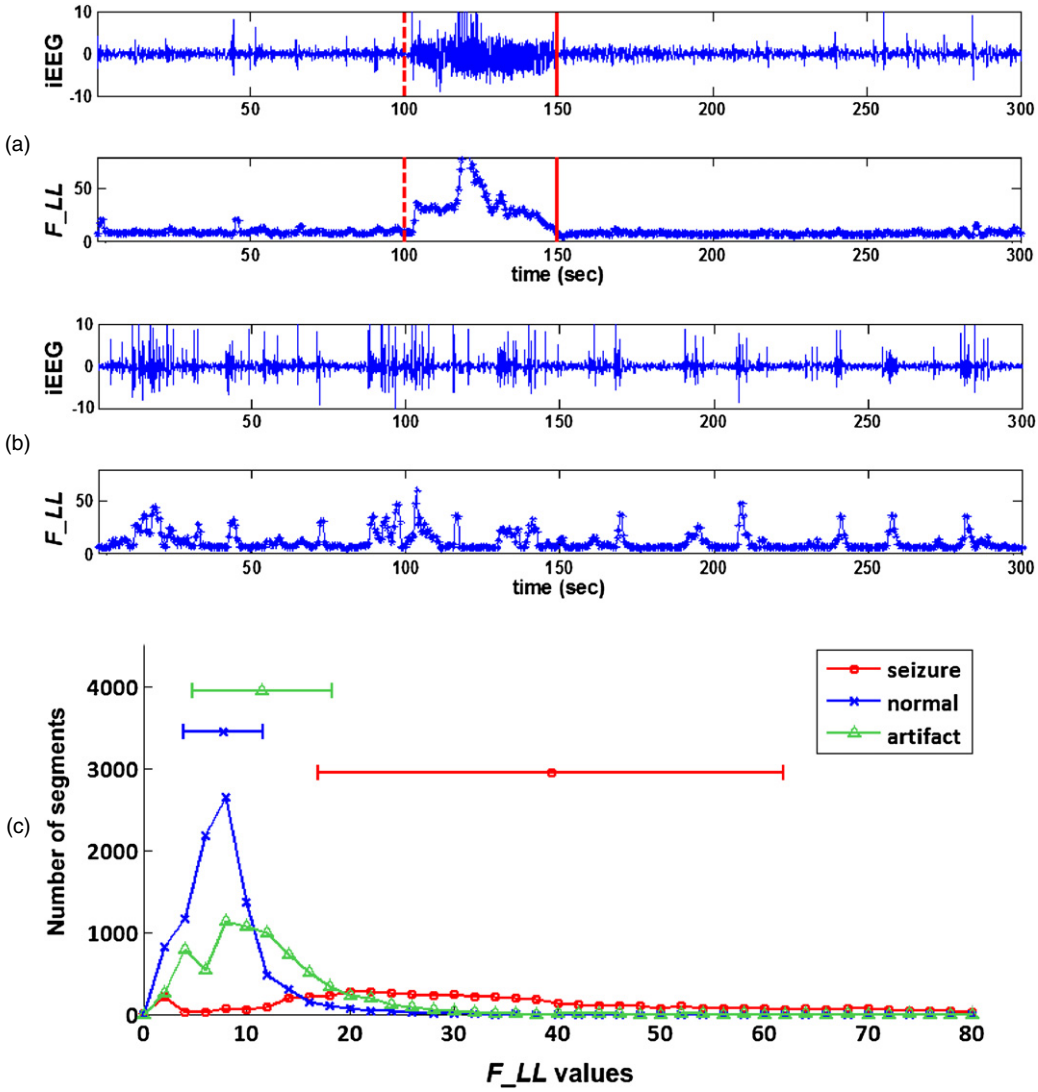

Figure 2. The examples of iEEG waveforms (a) with one seizure event and (b) seriously affected by artifacts when applying line length analysis. The row below the original iEEG displays its corresponding *F_LL* values. The dotted (solid) line indicates the time of seizure onset (end). (c) Histogram of *F_LL* for normal, seizure and artifact segments. The error bar for 'mean ± standard deviation' is also shown.

Based on the observation that the EEG pattern of a seizure is more ordered than that of a non-seizure, entropy has been used for seizure detection and analysis (Kannathal *et al* 2005, Ocak, 2009). To reduce the computational cost, *ApEn* (Pincus 1991) is used for real-time processing. Let the *N*-point time sequence of data equally spaced in time be $[u(1), u(2), \ldots, u(N)]$. First, for a sequence of vectors $\boldsymbol{x}(1)$, $\boldsymbol{x}(2), \ldots, \boldsymbol{x}(N–m+1)$ in $\boldsymbol{R}^m$,

$$x(i) = [u(i), u(i+1), \ldots, u(i+m-1)] \quad \text{for } 1 \leqslant i \leqslant (N-m+1), \tag{9}$$

where m is the length of the compared runs, we compare every vector pair, element by element. The vector comparison distance is defined as the maximum difference of the relative elements in two sequences $x(i)$ and $x(j)$:

$$\mathrm{d}[x(i), x(j)] = \max[|u(i+k) - u(j+k)|], \quad \text{for } k = 0, 1, \ldots, (m-1). \tag{10}$$

For each i, $1 \leqslant i \leqslant N-m+1$, we define

$$C_i^m(r) = \frac{\sum_{j=1}^{N-m+1} \omega_{i,j}}{N-m+1}, \tag{11}$$

where

$$\omega_{i,j} = \begin{cases} 1, & \text{if } d[x(i), x(j)] \leqslant r, \\ 0, & \text{else}, \end{cases} \tag{12}$$

and r is the tolerance of d. The approximate entropy, *ApEn*, is defined by

$$ApEn(m, r, N) = \Phi^m(r) - \Phi^{m+1}(r), \tag{13}$$

where

$$\Phi^m(r) = \frac{\sum_{i=1}^{N-m+1} \ln C_i^m(r)}{(N-m+1)}. \tag{14}$$

For the parameter setting of *ApEn*, we set that $m = 2$, $N = 128$ (0.5 s), and $r = 0.05$ for each patient. *ApEn* is a good index for discriminating between normal and ictal EEGs, but the *ApEn* values of the interictal EEGs overlap with those of the normal and the ictal EEGs (Liang *et al* 2010). Multi-band EEG power

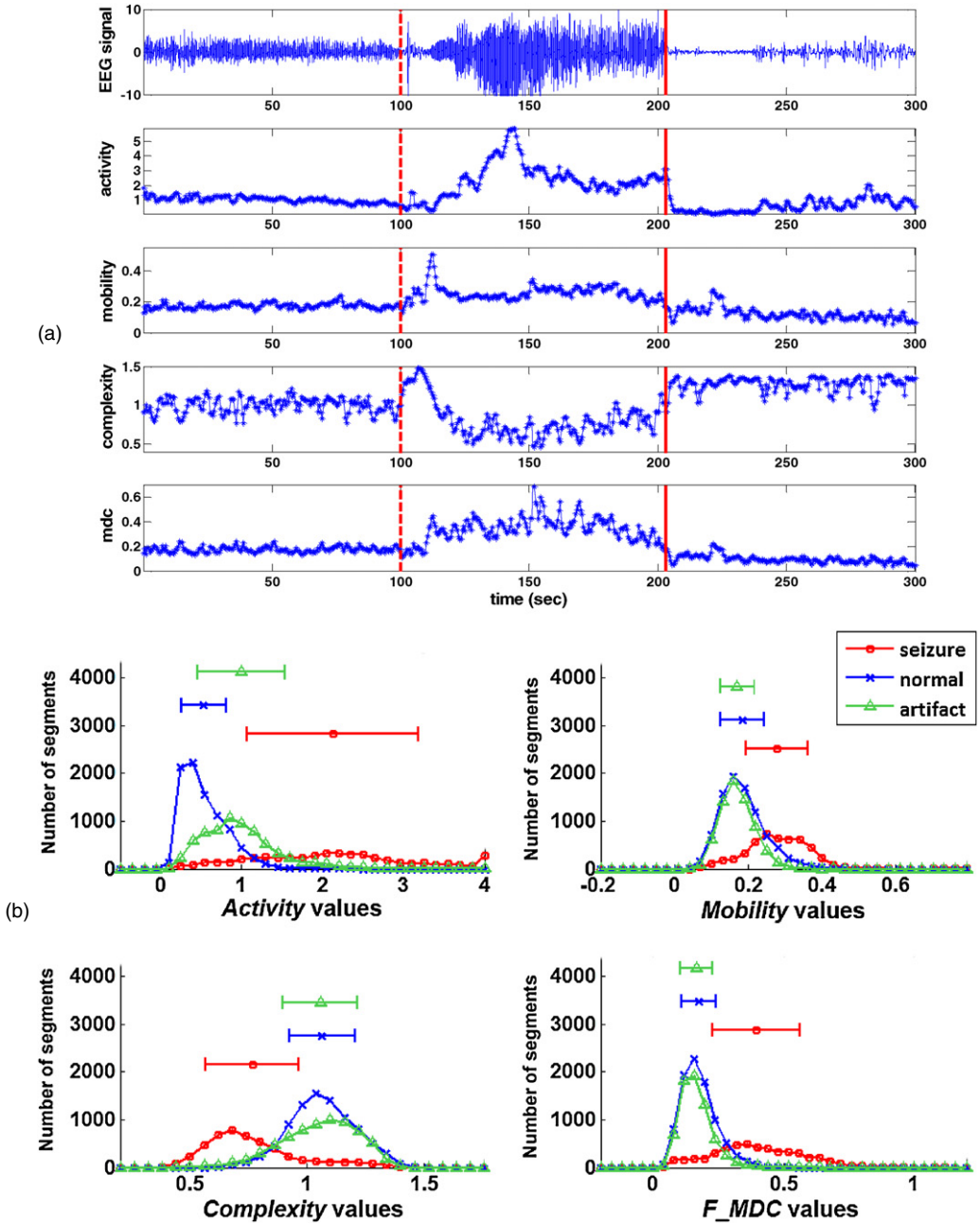

Figure 3. (a) The original iEEG waveforms and their Hjorth parameters of patient#21. The dotted line indicates the time of seizure onset at 100th s, and the solid line indicates the end of seizure. The second to fifth rows illustrate the analyzed signals by *Activity*, *Mobility*, *Complexity* and our proposed feature, '*F_MDC*'. (b) The histograms of four Hjorth parameters of normal, seizure and artifact segments. The error bar for 'mean ± standard deviation' is also shown.

spectra are therefore utilized as the complementary features of *ApEn* to reduce the false alarm rate. In this work, iEEG segments are filtered through a 0–60 Hz passband and the frequency band is divided into 15 sub-bands. The average EEG power of each sub-band is extracted as the spectral features. The spectral sub-band i, $0 \leqslant i \leqslant 14$, is calculated as follows:

$$F\_SSB_i = \text{Mean}[SSB(f)], \quad 4 \cdot i < f \leqslant 4 \cdot (i+1) \qquad (15)$$

where $SSB(f)$ is the power of the frequency band f (unit: Hz). Combining the *ApEn* feature, a total of 16 features are fed into the LDA for final confirmation.

The aim of the LDA is to use a hyper-plane to separate the data into different classes and to minimize the data distribution of the same class in the feature space (Lin *et al* 2008). For a two-class problem, the class of a feature vector depends on which side of the hyper-plane the vector is. The computational complexity of the LDA is relatively low and realizations in an embedded system have been presented (Hargrove *et al* 2010, Donohoo *et al* 2012). This algorithm is also successfully implemented on different processors for on-line detection of spontaneous absence seizures in animal models (Liang *et al* 2011, Young *et al* 2011) and in 24 h long-term uninterrupted EEG sequences (Chen *et al* 2011).

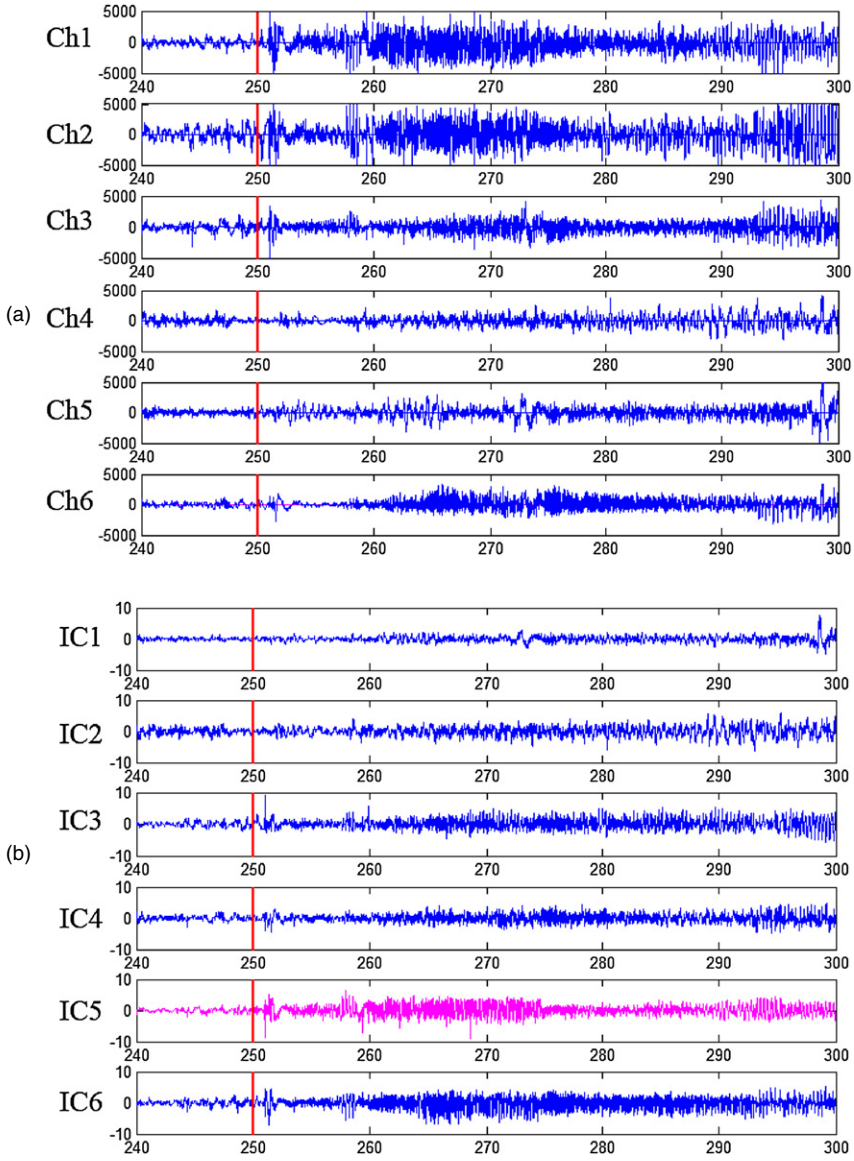

Figure 4. (a) The 6-channel iEEG waveforms with a seizure onset at the 250th s for patient#6; (b) The six ICs after FastICA decomposition.

2.6. Temporal constraint

To reduce the influence of iEEG fluctuations, a temporal constraint is used to make the final decision. In this study, the system outputs 1 for seizure and 0 for non-seizure every 0.25 s. If the number of consecutive windows classified as seizure by the second stage reaches a constant parameter *Nc*, a seizure event is claimed.

2.7. Strategy of cross validation

In this work, the leave-one-out cross validation is used to evaluate the generalization of the proposed system. When testing a certain patient's iEEG, the data of the other ten patients are used for training the model.

3. Results

Continuous iEEG data were screened by an expert and the seizure onset was defined as the onset of the epileptiform activity identified by the expert. The performance of the hierarchical approach is evaluated by three parameters: seizure detection accuracy, detection delay time, and false alarm rate (Aarabi *et al* 2009). Detection delay time is defined as the duration between the onset of an epileptiform activity scored by an expert and the time that the system reports. The seizure detection accuracy and the false alarm rate are defined as

$$\text{Detection accuracy} = \frac{TP}{TP + FN} \times 100\% \tag{16}$$

$$\text{False alarm rate} = FP/hr \tag{17}$$

where

true positive (TP): total number of correctly detected seizure events.

false negative (FN): total number of missed detections of seizure events.

false positive (FP): total number of non-seizure segments erroneously detected as seizure events.

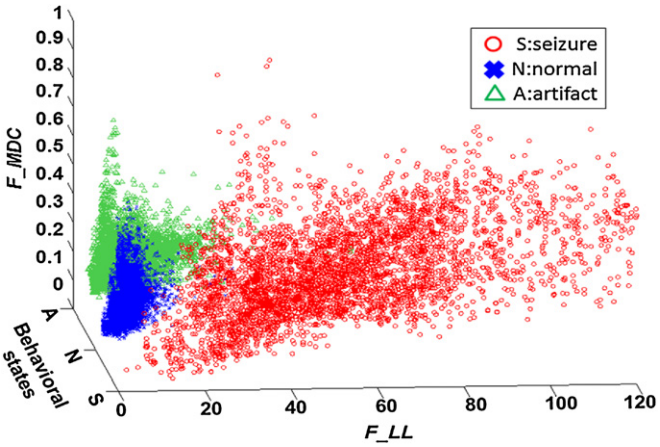

Figure 5. The 3D distribution of *F_LL* versus *F_MDC* of normal, seizure, and artifact EEG segments.

Table 2. The mixing matrix *A* of patient#6 and the resulting *R* ratios (sum of Ch1–Ch3/sum of Ch1–Ch6) of six ICs. The first three iEEG channels ($\alpha = 1$; $\beta = 2$; $\gamma = 3$) are closest to the seizure onset zone. Each column of *A* represents the projection of the certain IC onto the respective iEEG channels. The IC-5 has the highest ratio among all ICs and therefore it is chosen for further seizure detection.

	IC-1	IC-2	IC-3	IC-4	IC-5	IC-6
Ch-1 (α)	0.08	0.05	0.46	0.22	1.00	0.45
Ch-2 (β)	0.08	0.06	0.73	0.17	0.08	0.14
Ch-3 (γ)	0.17	0.02	0.12	0.53	0.70	0.62
Ch-4	0.86	1.00	0.08	0.70	0.23	0.01
Ch-5	1.00	0.42	0.07	0.45	0.04	0.02
Ch-6	0.20	0.03	1.00	1.00	0.03	1.00
Sum of Ch1–Ch3	0.33	0.13	1.31	0.92	1.78	1.21
Sum of Ch1–Ch6	2.39	1.58	2.46	3.07	2.08	2.24
Ratio (*R*)	0.14	0.08	0.53	0.30	0.86	0.54

The proposed detection method is verified on 11 epileptic patients who suffered from TLE. We first applied FastICA to 6-channel iEEGs to remove artifacts and extract the most seizure-related component. Taking patient #6 as an example, figure 4(a) shows that the original iEEG signals contain one seizure event of the subject, and figure 4(b) shows the six ICs after ICA decomposition. The resulting mixing matrix *A* is also shown in table 2, in which the first, second and third iEEG channels ($\alpha = 1$; $\beta = 2$; $\gamma = 3$) are closest to the seizure onset zone of the patient. Each column of *A* stands for the projection of each IC onto respective iEEG channels. It shows that IC-5 has the highest *R* value and is chosen for further seizure detection. Then, the signals of the determined IC are divided into 512-point segments (2 s) with an overlap size of 384 points (1.75 s). In the first stage, *F_LL* and *F_MDC* are applied as temporal constraints to detect the suspected seizure segments. A three-dimensional distribution of *F_LL* versus *F_MDC* of normal, seizure, and artifact iEEG segments is shown in figure 5. It can be seen that the non-seizure segments (marked as normal and artifact in figure 5) are distributed around the lower-left corner since they have insignificant values of *F_LL* and *F_MDC*. In contrast, the segments of seizures are distributed around the upper-right corner of the plot. That is, the *F_LL* and *F_MDC* values of seizure segments are almost higher than those of non-seizure segments. Table 3 shows the resulting values of *Th_1* and *Th_2* for each patient after the training phase. In the confirmation stage, a total of 16 features (from approximate entropy and 15 power bands) of a segment are used as input vectors to the LDA. When the LDA detects seizures for consecutive *Nc* segments, the system reports that a seizure occurs.

Table 3. The thresholds (*Th_1* and *Th_2*) used for each patient.

Patient	Th_1	Th_2
2	11.75	0.30
4	11.99	0.19
6	10.10	0.29
7	10.07	0.22
11	12.68	0.22
12	15.21	0.20
13	16.46	0.18
14	27.40	0.40
15	17.08	0.00
17	10.76	0.27
21	15.22	0.29

Table 4. Detection results for each patient. The performance was evaluated by three metrics: detection accuracy, false alarm rate, and detection delay time.

Patient	Total seizures	Detected seizures	Total testing EEG (h)	False alarm rate (# FP/h)	Delay (s)
2	3	3	5.54	0	7.2
4	5	5	24	0	5.3
6	3	3	24	0.21	5
7	3	3	24	0	3.7
11	4	3	24	0.04	3.2
12	4	4	24	0.08	1.9
13	2	2	24	0.08	5.5
14	4	4	24	0.21	28.1
15	4	4	24	0.13	18.4
17	5	5	24	0.13	10.9
21	5	4	24	0.13	12.1

Figure 6 presents an example of the detection result. The delay time of one seizure event for patient #4 is 4 s. Table 4 shows the experimental results for each patient. The proposed method misses two seizures, from patient#11 and patient#21. The detection accuracy achieves up to 95.24%. The false alarm rate ranges between 0 and 0.21 per hour, with an average of 0.09 per hour. The average delay time is 9.2 s with a standard deviation of 7.9 s.

Next, we verified the advantages contributed by the hierarchical detection method. We compared the results with only the fast detection stage (ST_1) and with the proposed two-stage algorithm (ST_{12}). When the number of consecutive seizure-like segments detected by the first stage reaches *Nc*, the system reports that a seizure occurs. Table 5 shows that the seizure detection accuracy of ST_1 is equal to ST_{12}, which both reached a detection accuracy of 95.24%. The delay time of ST_1 is 8.8 s with a standard deviation of 7.9 s, which is also similar to that of ST_{12}. Without the confirmation stage, however, the average false alarm rate for all patients raises to 0.72/h, which is eight times higher than the proposed method. It is proved that the second stage can significantly reduce the false alarm rate.

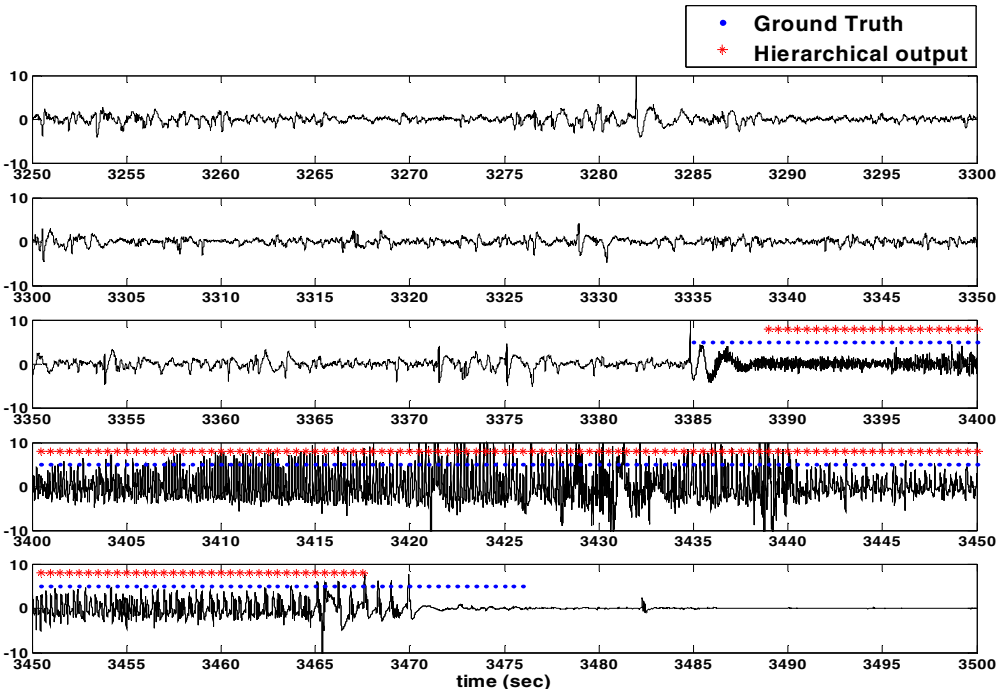

Figure 6. The detection results of one seizure event for patient#4. The dots indicate the seizure events labeled by an expert, while stars denote the results detected by the proposed system. The detection delay time is 4.0 s.

Table 5. Performance comparison for two detection methods: fast suspect detection with only one stage (ST_1) and two-stage detection (ST_{12}). Standard deviations are listed in parenthesis.

Patient	Stage	Total seizures	Detected seizures	False detection	Total testing EEG (h)	False alarm rate (# FP/h)	Average delay time (s)
2	ST_1	3	3	11	5.54	1.99	6.7
	ST_{12}		3	0		0	7.2
4	ST_1	5	5	16	24	0.67	4.8
	ST_{12}		5	0		0	5.3
6	ST_1	3	3	15	24	0.63	4.7
	ST_{12}		3	5		0.21	5
7	ST_1	3	3	11	24	0.46	3.7
	ST_{12}		3	0		0	3.7
11	ST_1	4	3	1	24	0.04	3.2
	ST_{12}		3	1		0.04	3.2
12	ST_1	4	4	3	24	0.13	1
	ST_{12}		4	2		0.08	1.9
13	ST_1	2	2	9	24	0.38	5.5
	ST_{12}		2	2		0.08	5.5
14	ST_1	4	4	69	24	2.88	28
	ST_{12}		4	5		0.21	28.1
15	ST_1	4	4	7	24	0.29	17.8
	ST_{12}		4	3		0.13	18.4
17	ST_1	5	5	5	24	0.21	9
	ST_{12}		5	3		0.13	10.9
21	ST_1	5	4	5	24	0.21	12.1
	ST_{12}		4	3		0.13	12.1
Total	ST_1	42	40	152	245.54	X	X
	ST_{12}		40	24			
Avg.	ST_1	X	95.24%	13.8(18.9)	22.3 (5.6)	0.72 (0.9)	8.8 (7.9)
	ST_{12}		95.24%	2.2 (1.8)	22.3 (5.6)	0.09 (0.1)	9.2 (7.9)

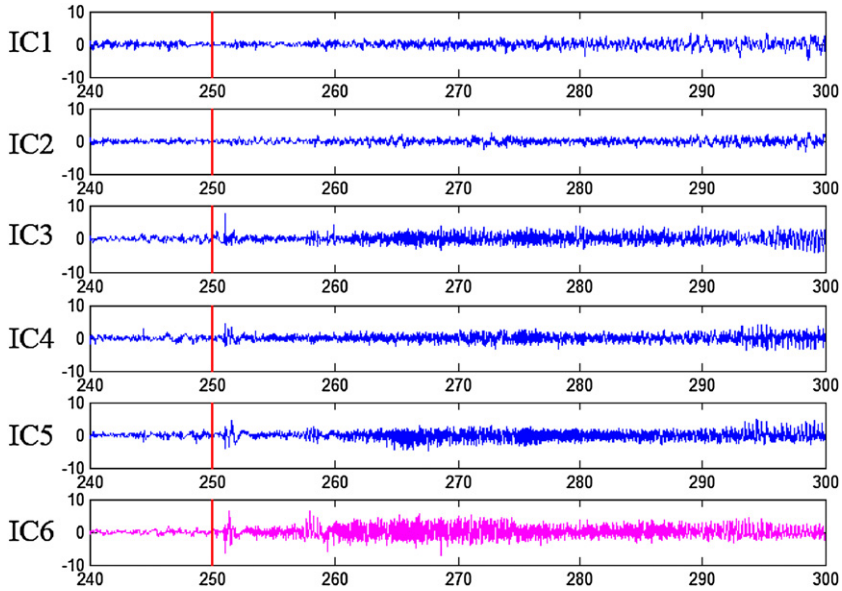

Figure 7. The six ICs decomposed by applying ICA to the segment containing the first seizure event of patient#6.

The fast suspect detection is a low-complexity seizure detection method. Only two temporal features, *F_LL* and *F_MDC*, are used to detect the state of iEEG segment: seizure or non-seizure. The second stage is developed for final confirmation to reduce the false alarm rate. The proposed approach consists of line length analysis, Hjorth analysis, approximate entropy, and LDA classification. It can be easily implemented on hardware with current processing platforms. Unlike patient-specific methods, the proposed seizure detection method can be applied across patients for real-time demands.

Table 6. The mixing matrix A_1 of patient#6 obtained by applying ICA to the segment containing the first seizure event.

	IC-1	IC-2	IC-3	IC-4	IC-5	IC-6
Ch-1	0.06	0.04	0.28	0.39	0.10	1.00
Ch-2	0.08	0.05	0.60	0.15	0.20	0.07
Ch-3	0.06	0.00	0.01	1.00	0.64	0.32
Ch-4	1.00	0.85	0.16	0.71	0.17	0.08
Ch-5	0.02	1.00	0.04	0.37	0.10	0.04
Ch-6	0.04	0.07	1.00	0.70	1.00	0.53
Ratio	0.16	0.04	0.43	0.46	0.43	0.68

4. Discussion

An on-line seizure detection system can drive an antiepileptic stimulator in real time to suppress seizures (Stacey and Litt 2008). This work develops an on-line seizure detection method that can be applied to monitor continuous iEEG signals of patients who suffered from TLE. The results show that the proposed method has superior performance on leave-one-out subject independent evaluation. The average detection accuracy, false alarm rate, and delay time are 95.24%, 0.09/h, and 9.2 s, respectively.

In previous studies that analyzed the same database, the line length (Esteller *et al* 2001) or spike rate (Schad *et al* 2008) was used as a simple threshold to detect a seizure; Meier *et al* (2008) and Liu *et al* (2012) applied a support vector machine (SVM) to classify the state of an iEEG's segment; Aarabi *et al* (2009) used a fuzzy-rule based classifier; Zhang *et al* (2010) proposed a patient-specific seizure onset detection method based on incremental non-linear dimensionality reduction. The detection accuracies range between 62% and 98.8% and the false alarm rates are between 0.15 and 0.58 per hour. The average delays range from 10.8 to 12.3 s, except for the method proposed by Meier *et al* (2008), whose average delay is 1.6 s at the cost of a false alarm rate of 0.45 per hour. The proposed hierarchical approach has comparable performance on the detection accuracy and achieves the lowest false alarm rate among the existing methods.

In this study, we propose an independent component (IC) selection strategy to automatically determine the most seizure-related IC for seizure detection. Experimental results show that it can effectively reduce the false alarm rate by extracting meaningful features and eliminating artifacts. Because the mixing matrix can be predetermined, we further evaluate the reproducibility of the determined IC. Taking the data from patient#6, we apply ICA to the segment that contains only the first seizure event. The six ICs after ICA decomposition are shown in figure 7, in which A_1 and A represent the ICA results of the segment containing the first seizure event and the whole segment, respectively. The resulting mixing matrix of A_1 is shown in table 6. IC-6 is selected since it has the highest R value. Comparing table 6 with table 2 and figure 7 with figure 4(b), respectively, it is observed that IC-6 of A_1 and IC-5 of A contain the most ictal activities and Ch-1 of the original recording has the strongest correlation with these two ICs. Figure 8 shows that the ICs during the same period contain the second seizure event of patient#6. Figures 8(a) and 8(b) depict the ICs of A_1 and A, as listed in tables 6 and 2, respectively. The signals of IC-6 in figure 8(a) and IC-5 in figure 8(b) contain stronger seizure waveforms after seizure onset (800–815 s) compared with the other ICs. Analysis on other

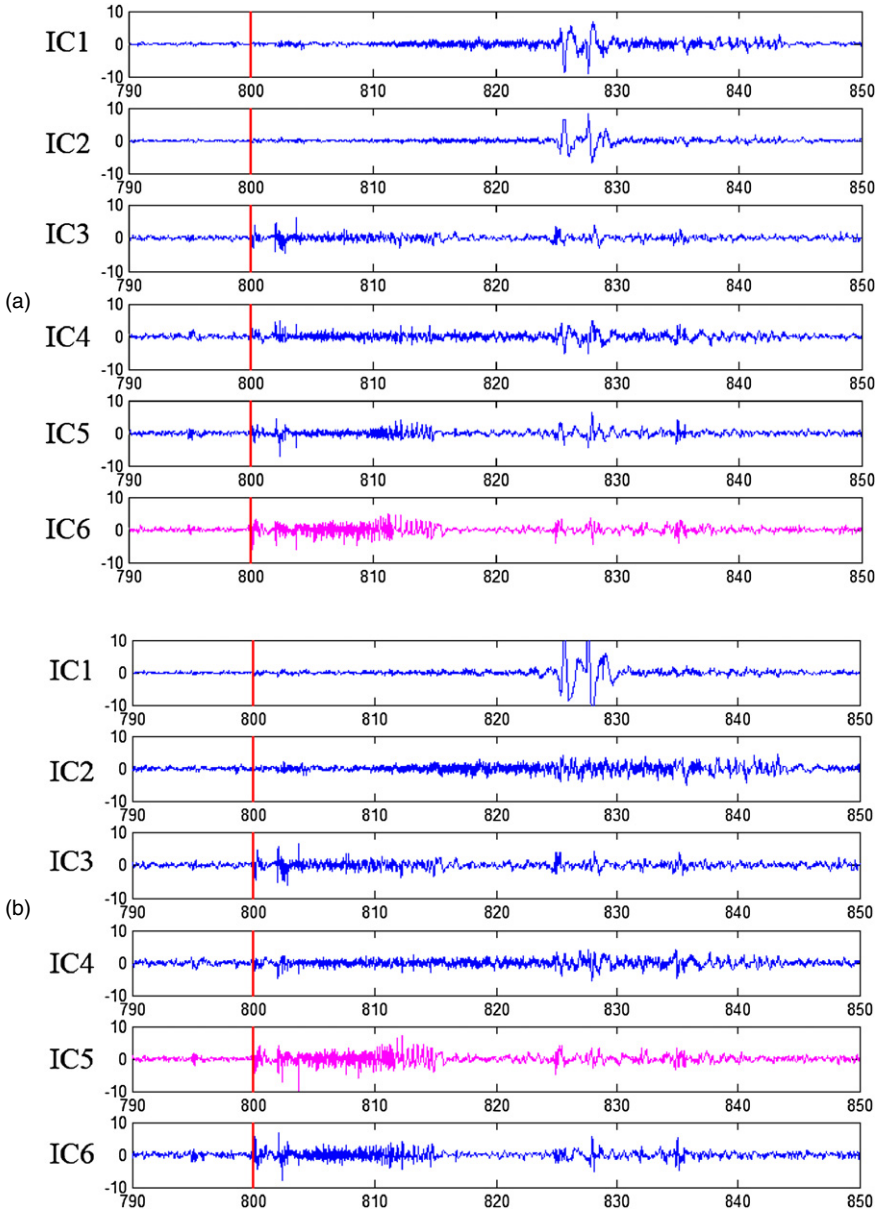

Figure 8. The IC signals during the period containing the second seizure event of patient#6. Plots (a) and (b) show the signals of IC decomposed by A_1 (table 6) and A (table 2), respectively.

subjects is shown in table 7. Only the vectors corresponding to the selected ICs are shown. It is found that the determined ICs from A_1 and A for each patient have stronger correlations on the same channel, although these ICs are obtained from different iEEG segments. This verifies the reproducibility of the selected IC on the utilized database. In addition to off-line ICA, we are also developing an on-line ICA chip to deal with the drift of iEEG signals due to long-term medication or the use of closed-loop seizure controllers (Chen *et al* 2012, Liang *et al* 2011). The proposed IC selection strategy can be applied to these applications.

The ICA pre-processing and temporal constraint strategy used in our approach effectively reduces the false detections caused by the influence of unexpected signal variability and/or artifacts. There is a fundamental tradeoff between accuracy, delay time, and false alarm rate in setting the parameters for seizure detection. The number of consecutive windows *Nc* for seizure detection is set to 6 in this work so that the minimum delay time is 1.5 s. An increased *Nc* results in a reduced false alarm rate and an increased detection delay. On the contrary, a decreased *Nc* causes an increased false alarm rate. Figure 9 shows the performance of the proposed seizure detection method for various values of *Nc*: $Nc = 1, 2, 4, 6, 8$ to 10. Without temporal constraint (i.e. $Nc = 1$), integrating entropy and the spectral features of EEG signals along with a linear classifier can achieve a 100% detection accuracy and the average delay time is less than 6 s, at the cost of a false alarm rate of up to 15.8 FP/h. When $Nc = 10$ is applied, the false alarm rate reduces to 0.03. However, the detection accuracy decreases to 90% and the detection delay increases to 14 s accordingly.

Table 8 summarizes the detection results of the proposed method with respect to different seizure types, origins, and

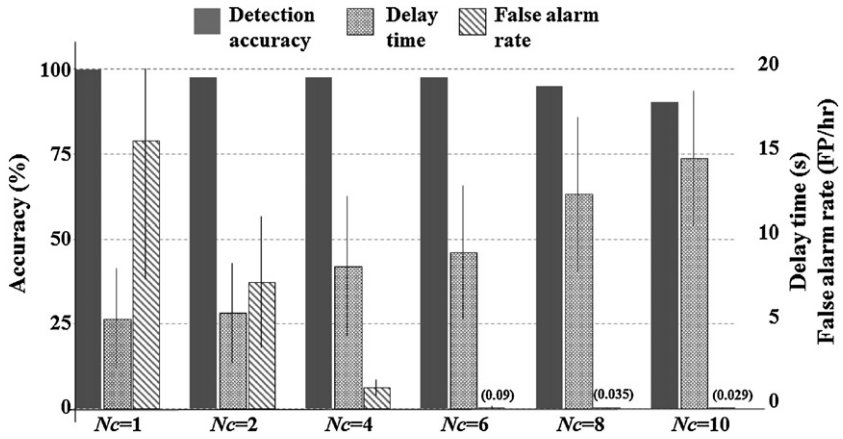

Figure 9. The performance of accuracy, delay time and false alarm rate when various values of *Nc* are applied. The lines are expressed as 'mean ± 0.5*standard deviation'.

Table 7. The vectors (in the mixing matrices A_1 and A) corresponding to the selected ICs for 10 patients with TLE in this study.

	Patient#2		Patient#4		Patient#7		Patient#11		Patient#12	
	A_1	A	A_1	A	A_1	A	A_1	A	A_1	A
Ch-1	0.73	0.48	0.96	0.85	0.10	0.41	0.00	0.02	1.00	1.00
Ch-2	1.00	1.00	0.05	0.12	0.25	0.35	0.02	0.21	0.47	0.20
Ch-3	0.25	0.01	1.00	1.00	1.00	1.00	1.00	1.00	0.71	0.66
Ch-4	0.00	0.25	0.02	0.08	0.02	0.00	0.08	0.11	0.08	0.06
Ch-5	0.03	0.07	0.01	0.00	0.04	0.07	0.01	0.23	0.10	0.04
Ch-6	0.03	0.02	0.00	0.02	0.17	0.14	0.03	0.15	0.16	0.00
Ratio	0.96	0.81	0.98	0.95	0.86	0.89	0.89	0.71	0.87	0.95
	Patient#13		Patient#14		Patient#15		Patient#17		Patient#21	
	A_1	A	A_1	A	A_1	A	A_1	A	A_1	A
Ch-1	1.00	1.00	0.15	0.78	1.00	1.00	0.72	0.21	1.00	1.00
Ch-2	0.73	0.95	1.00	1.00	0.14	0.09	0.70	0.82	0.00	0.29
Ch-3	0.21	0.05	0.03	0.01	0.11	0.89	1.00	1.00	0.04	0.04
Ch-4	0.02	0.01	0.05	0.34	0.08	0.01	0.02	0.01	0.03	0.00
Ch-5	0.00	0.01	0.00	0.03	0.09	0.12	0.01	0.01	0.00	0.29
Ch-6	0.71	0.00	0.03	0.00	0.10	0.16	0.02	0.04	0.03	0.35
Ratio	0.73	0.99	0.93	0.83	0.82	0.87	0.98	0.97	0.94	0.67

Table 8. Analysis of detection results with respect to seizure type, origin, and resection outcome.

Seizure type				
	Number of subjects	Detection accuracy (%)	False alarm rate (FP/hr)	Delay time (s)
Simple partial seizures	9	94.5%	0.06 ± 0.05	7.6 ± 5.3
Complex partial seizure	11	95.2%	0.09 ± 0.08	9.2 ± 7.9
Generalized tonic–clonic seizures	10	97.3%	0.09 ± 0.08	8.9 ± 8.3
Origin				
	Number of subjects	Detection accuracy (%)	False alarm rate (FP/hr)	Delay time (s)
Hippocampus	6	100.0%	0.06 ± 0.08	4.8 ± 1.8
Neocortex	3	85.7%	0.10 ± 0.05	8.7 ± 4.8
Hippocampus and Neocortex	2	100.0%	0.17 ± 0.06	23.2 ± 6.9
Resection outcome				
	Number of subjects	Detection accuracy (%)	False alarm rate (FP/hr)	Delay time (s)
Class I and II	7	92.3%	0.11 ± 0.08	9.8 ± 8.8
Class III and IV	3	100.0%	0.07 ± 0.07	9.1 ± 8.4

resection outcomes. The proposed method outputs stable results for a variety of seizure types and resection outcomes, but its performance depends on the origins. For the origins, this method yields the best performance on the six patients with mesial TLE of hippocampal origin (patient#2, #4, #6, #7, #12 and #13) in terms of detection accuracy, false alarm rate, and delay time. There are two missed detections in the neocortical group (patient#11 and #21). Although seizures from patients with TLE of hippocampal and neocortical origin are 100% detected, the detection delay is 23.2 s on average.

A seizure detection system that can monitor long-term continuous EEG signals of epileptic patients is essential for closed-loop seizure control and pre-surgical monitoring. For implantable or wearable devices, the battery life of such a detection system becomes important. Power consumption can be saved through the use of a power-efficient hardware computing platform. Chen *et al* (2011) carried out a real-time seizure detection system based on reduced instruction set computer (RISC) architecture. The measurement results show that the RISC architecture can reduce over 90% power consumption compared with its previous prototype, which was implemented on an enhanced 8051 microprocessor (Liang *et al* 2011). Given a computing platform, the energy can be further saved by using an improved detection algorithm. This work proposes a two-stage method of energy saving. The first stage fast detects the suspected seizure segment. Due to the low-complexity algorithm, it can be operated with less power dissipation. The engine of seizure confirmation stays idle until the suspected seizure segment is detected. For the database used in this work, the length of iEEG recordings for 11 patients is 245.54 h. Without the fast suspect detection, the engine needs to keep running all along. With the proposed hierarchical detection algorithm, the engine only operates to detect seizures for 1.72 h for all patients. The execution time is saved by 99.3% in this experiment. In this way, the sustainability of the closed-loop seizure control system can be improved. The energy savings depend on the occurrence of seizures in patients. Better energy savings are achieved for patients with mild or moderate seizure occurrences.

EEG onset is defined as a sustained rhythmic change in the brain's activity accompanied by subsequent clinically typical seizure activity (Lee *et al* 2000). Instead of detecting seizures after clinical onset, our system detects the seizures after EEG onset. The duration between EEG seizure onset and clinical seizure onset is an important issue to discover. It was reported that the EEG seizure onset precedes clinical seizure onset by at least 11.7 s in patients with refractory TLE (Weinand *et al* 2007). Our system can detect the seizures 9.2 s after EEG seizure onset on average, which is shorter than the results reported in Weinand *et al* (2007). This makes an early detection of seizure events before the clinical seizure activity possible. However, how early an anti-epileptic device could effectively control clinical seizures is still under investigation.

The discrimination of vigilance states is very important, and it helps us to understand the functional relationship between brain and behavior. A combination of video and EEG is commonly used in the clinic, but the video provides low spatial- and temporal-resolution for the study of brain-behavior association. Recently, we have presented a multi-channel wireless system for monitoring the EEG signals of freely moving rats, and TLE detection is performed through a combination of EEG and an accelerometer (Chang *et al* 2011, Wang *et al* 2012). We have confirmed its performance by video examination and demonstrated the improved accuracy of discrimination in a vigilance stage. If accelerometers can be integrated into our proposed system, the detection delay time would be further reduced.

In the future, this method will be implemented in our closed-loop seizure controller (Liang *et al* 2011) for suppression of temporal lobe seizures. Because the developed method has low computational complexity and high detection accuracy, it can be integrated with an electrical stimulator or drug delivery device to perform closed-loop seizure control to enhance the patients' quality of life. In conjunction with wireless transmission, the maximum portability and wearability of the seizure control system can be achieved (Young *et al* 2011, Liang *et al* 2011). In addition to off-line ICA, we are also developing an on-line ICA chip to deal with the drift of iEEG signals due to long-term medication or the use of closed-loop seizure controllers (Chen *et al* 2012). The proposed IC selection strategy can also be applied to these applications. We also plan to discover the longest stimulation delay, after the EEG onset, to suppress seizures successfully in animal models.

Acknowledgments

This work was supported by the National Science Council of Taiwan under Grants NSC-101-2220-E-006-010 and NSC-98-2221-E-006-161-MY3.

References

Aarabi A, Fazel-Rezai R and Aghakhani Y 2009 A fuzzy rule-based system for epileptic seizure detection in intracranial EEG *Clin. Neurophysiol.* **120** 1648–57

Aschenbrenner-Scheibe R, Maiwald T, Winterhalder M, Voss H U, Timmer J and Schulze-Bonhage A 2003 How well can epileptic seizures be predicted? An evaluation of a nonlinear method *Brain* **126** 2616–26

Ayoubian L, Lacoma H and Gotman J 2013 Automatic seizure detection in SEEG using high frequency activities in wavelet domain *Med. Eng. Phys.* **35** 319–28

Chabardes S, Kahane P, Minotti L, Koudsie A, Hirsch E and Benabid A L 2002 Deep brain stimulation in epilepsy with particular reference to the subthalamic nucleus *Epileptic Disord.* **4** (Suppl. 3) S83–93

Chang H Y, Yang S C, Lan S H and Chung P C 2010 Epileptic seizure detection in grouped multi-channel EEG signal using ICA and wavelet transform *IEEE Int. Symp. on Circuits and Systems* pp 1388–91

Chen T J, Chiueh H, Liang S F, Chang S T, Jeng C, Hsu Y and Chien T C 2011 The implementation of a low-power biomedical signal processor for real-time epileptic seizure detection on absence animal models *IEEE J. Emerg. Sel. Top. Circuits Syst.* **1** 613–21

Chen T J, Shih Y H, Yang C H, Chiueh H and Liang S F 2012 A low-power signal processor with an ICA engine for real-time epileptic seizure detection *Neural Interfaces Conf.* p 116

Donohoo B, Ohlsen C, Pasricha S and Anderson C 2012 Exploiting spatiotemporal and device contexts for energy-efficient mobile embedded systems *Des. Automat. Conf. (DAC)* pp 1274–9

Engel J 1989 *Seizure and Epilepsy* (Philadelphia PA: Davis)

Esteller R, Echauz J and Tcheng T 2004 Comparison of line length feature before and after brain electrical stimulation in epileptic patients *Conf. Proc. IEEE Eng. Med. Biol. Soc.* **2** 4710–3

Esteller R, Echauz J, Tcheng T, Litt B and Pless B 2001 Line length: an efficient feature for seizure onset detection *Int. Conf. IEEE Eng. Med. Biol. Soc.* **2** 1707–10

Freiburg Seizure Prediction Project 2008 Freiburg, Germany (https://epilepsy.uni-freiburg.de/)

Hargrove L J, Scheme E J, Englehart K B and Hudgins B S 2010 Multiple binary classifications via linear discriminant analysis

for improved controllability of a powered prosthesis *IEEE Trans. Neural Syst. Rehabil. Eng.* **18** 49–57
Hjorth B 1970 EEG analysis based on time domain properties *Electroencephalogr. Clin. Neurophysiol.* **29** 306–10
Hyvärinen A 1999 Fast and robust fixed-point algorithms for independent component analysis *IEEE Trans. Neural Netw.* **10** 626–34
Indiradevi K P, Elias E and Sathidevi P S 2009 Complexity analysis of electroencephalogram records of epileptic patients using Hurst exponent *Int. J. Med. Eng. Inform.* **1** 368–80
Jung T P, Makeig S, Westerfield M, Townsend J, Courchesne E and Sejnowski T 2000 Removal of eye activity artifacts form visual event-related potential in normal and clinical subjects *Clin. Neurophysiol.* **111** 1745–58
Kannathal N, Choo M L, Acharya U R and Sadasivan P K 2005 Entropies for detection of epilepsy in EEG *Comput. Methods Programs Biomed.* **80** 187–94
Kocyigit Y, Alkan A and Erol H 2008 Classification of EEG recordings by using fast independent component analysis and artificial neural network *J. Med. Syst.* **32** 17–20
Kossoff E H, Ritzl E K, Politsky J M, Murro A M, Smith J R, Duckrow R B, Spencer D D and Bergey G K 2004 Effect on external responsive neurostimulator on seizures and electrographic discharges during subdural electrode monitoring *Epilepsia* **45** 1560–67
Labar D, Murphy J and Tecoma E 1999 Vagus nerve stimulation for medication-resistant generalized epilepsy *Neurology* **52** 1510–2
Lee S A, Spencer D D and Spencer S S 2000 Intracranial EEG seizure-onset patterns in neocortical epilepsy *Epilepsia* **41** 297–307
LeVan P, Urrestarazu E and Gotman J 2006 A system for automatic artifact removal in ictal scalp EEG based on independent component analysis and Bayesian classification *Clin. Neurophysiol.* **117** 912–27
Liang S F, Wang H C and Chang W L 2010 Combination of EEG complexity and spectral analysis for epilepsy diagnosis and seizure detection *EURASIP J. Adv. Signal Process.* **2010** 853434
Liang S F, Liao Y C, Shaw F Z, Chang D W, Young C P and Chiueh H 2011 Closed-loop seizure control on epileptic rat models *J. Neural Eng.* **8** 045001
Lin C T, Lin K L, Ko L W, Liang S F, Kuo B C and Chung I F 2008 Nonparametric single-trial EEG feature extraction and classification of driver's cognitive responses *EURASIP J. Appl. Signal Process.* **2008** 849040
Liu Y, Zhou W, Yuan Q and Chen S 2012 Automatic seizure detection using wavelet transform and SVM in long-term intracranial EEG *IEEE Trans. Neural Syst. Rehabil. Eng.* **20** 749–55
McMenamin B W, Shackman A J, Maxwell J S, Bachhuber D R, Koppenhaver A M, Greischar L L and Davidson R J 2010 Validation of ICA-based myogenic artifact correction for scalp and source-localized EEG *NeuroImage* **49** 2416–32
Meier R, Dittrich H, Schulze-Bonhage A and Aertsen A 2008 Detecting epileptic seizures in long-term human EEG: a new approach to automatic online and real-time detection and classification of polymorphic seizure patterns *J. Clin. Neurophysiol.* **25** 119–31
Ocak H 2009 Automatic detection of epileptic seizures in EEG using discrete wavelet transform and approximate entropy *Expert Syst. Appl.* **36** 2027–36
Osorio I *et al* 2002 Performance reassessment of a real-time seizure-detection algorithm on long ECoG series *Epilepsia* **43** 1522–35
Päivinen N, Lammi S, Pitkanen A, Nissinen J, Penttonen M and Gronfors T 2005 Epileptic seizure detection: a nonlinear viewpoint *Comput. Methods Programs Biomed.* **79** 151–9
Pincus S M 1991 Approximate entropy as a measure of system complexity *Proc. Natl Acad. Sci. USA* **88** 2297–301
Politsky J M, Estellar R, Murro A M, Smith J R, Ray P, Park Y D and Morrell M J 2005 Effects of electrical stimulation paradigm on seizure frequency in medically intractable partial seizure patients with a cranially implanted responsive cortical neurostimulator *Proc. Annu. Meeting Am. Epilepsy Soc.* Abst 3.167
Raghunathan S, Gupta S K, Ward M P, Worth R M, Roy K and Irazoqui P P 2009 The design and hardware implementation of a low-power real-time seizure detection algorithm *J. Neural Eng.* **6** 056005
Schad A, Schindler K, Schelter B, Maiwald T, Brandt A, Timmer J and Schulze-Bonhage A 2008 Application of a multivariate seizure detection and prediction method to non-invasive and intracranial long-term EEG recordings *Clin. Neurophysiol.* **119** 197–211
Stacey W C and Litt B 2008 Technology insight: neuroengineering and epilepsy—designing devices for seizure control *Nat. Clin. Pract. Neurol.* **4** 190–201
Subasi A and Gursoy M 2010 EEG signal classification using PCA, ICA, LDA and support vector machines *Expert Syst. Appl.* **37** 8659–66
Wang Y L, Liang S F, Shaw F Z, Su A W Y, Chen Y L and Wu S Y 2012 Use of accelerometers to detect motor states in a seizure of rats with temporal lobe epilepsy *IEEE BioCAS* pp 372–5
Weinand M, Farley C, Hussain N, Labiner D and Ahern G 2007 Time from ictal subdural EEG seizure onset to clinical seizure onset: an electrocorticographic time factor associated with temporal lobe epileptogenicity *Neurol. Res.* **29** 862–70
White A M, Williams P A, Ferraro D J, Clark S, Kadam S D, Dudek F E and Staley K J 2006 Efficient unsupervised algorithms for the detection of seizures in continuous EEG recordings from rats after brain injury *J. Neurosci. Methods* **152** 255–66
Wilson S B 2006 Algorithm architectures for patient dependent seizure detection *Clin. Neurophysiol.* **117** 1204–15
Young C P, Liang S F, Chang D W, Liao Y C, Shaw F Z and Hsieh C H 2011 A portable wireless on-line closed-loop seizure controller in freely moving rats *IEEE Trans. Instrum. Meas.* **60** 513–21
Zhang Y, Xu G, Wang J and Liang L 2010 An automatic patient-specific seizure onset detection method in intracranial EEG based on incremental nonlinear dimensionality reduction *Comput. Biol. Med.* **40** 889–99